Redox Biology 84 (2025) 103704

Contents lists available at ScienceDirect

Redox Biology

journal homepage: www.elsevier.com/locate/redox

# Ubiquitin-specific protease 38 exacerbates diabetic cardiomyopathy via post-translational modification of ACAD11

Zheng Xiao [a,b,c,1], Yucheng Pan [a,b,c,1], Hong Meng [a,b,c], Zongze Qu [a,b,c], Liang Guo [a,b,c], Bin Kong [a,b,c], Wei Shuai [a,b,c,*], He Huang [a,b,c,**]

[a] Department of Cardiology, Renmin Hospital of Wuhan University, Wuhan, China
[b] Hubei Key Laboratory of Cardiology, Wuhan, China
[c] Cardiovascular Research Institute of Wuhan University, Wuhan, China

ARTICLE INFO

*Keywords:*
Diabetic cardiomyopathy
Ubiquitin-specific protease 38
Mitochondrial dysfunction
Acyl-CoA dehydrogenase 11
Receptors of advanced glycemic end products

ABSTRACT

*Background:* Diabetic cardiomyopathy (DCM) is a prevalent and severe complication of diabetes, for which effective management strategies remain limited. Ubiquitin-specific protease 38 (USP38) has been associated with various cardiovascular diseases. In this study, we investigate the role of USP38 in the pathogenesis of DCM.
*Methods:* Cardiomyocyte-specific transgenic and knockout USP38 mice were generated, and diabetic mouse model was established using streptozotocin injections. Neonatal rat cardiomyocytes exposed to high glucose conditions were utilized for in vitro experiments. Cardiac remodeling was assessed through echocardiography, electrophysiological analysis, histological assessment, and molecular analysis.
*Results:* USP38 expression was significantly upregulated in DCM. Cardiomyocyte-specific USP38 overexpression aggravated cardiac dysfunction, cardiac inflammation and myocardial fibrosis, mitochondrial dysfunction, and increased vulnerability to ventricular arrhythmia in diabetic mice. Conversely, cardiomyocyte-specific USP38 deletion improved cardiac structural and electrical remodeling and attenuated mitochondrial impairment. Similar results were observed in vitro. Mechanistically, RNA-sequencing analysis, immunoprecipitation and mass spectrometry analysis and lipidomic analysis demonstrated that USP38 directly interacts with Acy-CoA dehydrogenase (ACAD11), deubiquitinating and inactivating it. This leads to abnormal fatty acid oxidation and subsequent activation of the receptor for advanced glycation end products (RAGE) pathway in diabetic heart. Pharmacological inhibition of RAGE using FPS-ZM1 hampered cardiac remodeling and dysfunction in cardiomyocyte-specific USP38 overexpressing diabetic mice.
*Conclusion:* The study demonstrates that USP38 exacerbates diabetes-induced cardiac remodeling and DCM via post-translational modification of ACAD11, highlighting a novel therapeutic target for DCM.

## 1. Introduction

The global prevalence of diabetes mellitus is rising rapidly, placing significant burden on public health worldwide [1]. Diabetic cardiomyopathy (DCM), a serious complication of diabetes, is characterized by both diastolic and systolic dysfunction, which can eventually lead to heart failure (HF) [2–4]. Furthermore, DCM has been reported to increase the risk of fatal ventricular arrhythmias (VAs) [5]. Despite this, effective therapeutic strategies for DCM remain limited, and glycemic control along often fails to improve cardiac function or long-term outcomes. Therefore, it is particularly important to find novel therapeutic option for DCM.

The progression of DCM is driven by a range of pathological mechanisms, including inflammation, oxidative stress, mitochondrial dysfunction, impaired insulin metabolic signaling and cardiac autonomic neuropathy, etc [6]. Among these, alternations in myocardial energy metabolism have attracted increasing attention. Cardiomyocytes are high energy consuming cells, and under physiological conditions,

* Corresponding author. Department of Cardiology, Renmin Hospital of Wuhan University, 238 Jiefang Road, Wuhan 430060, Hubei, China.
** Corresponding author. Department of Cardiology, Renmin Hospital of Wuhan University, 238 jiefang Road, Wuhan 430060, Hubei, China.
*E-mail addresses:* sw09120@whu.edu.cn (W. Shuai), huanghe1977@whu.edu.cn (H. Huang).
[1] Zheng Xiao and Yucheng Pan contributed equally.

https://doi.org/10.1016/j.redox.2025.103704
Received 16 May 2025; Accepted 27 May 2025
Available online 28 May 2025

40–60 % of energy supply of cardiomyocytes is derived from fatty acid β-oxidation [7]. In diabetic hearts, there is a significant shift in myocardial energy metabolism, with increased reliance on fatty acid oxidation and reduced glucose utilization [8]. This metabolic imbalance contributes to mitochondrial dysfunction, impaired ATP production, and worsened cardiac dysfunction.

Acyl-CoA dehydrogenases (ACADs) play a crucial role in the dehydrogenation process during fatty acid oxidation. Well-established members of this family, such as very long chain acyl-CoA dehydrogenase (VLCAD), medium-chain acyl-CoA dehydrogenase (MCAD), and short-chain acyl-CoA dehydrogenase (SCAD),participate in the metabolism of long-chain to medium-chain and finally to short-chain acyl-CoAs [9,10]. Recently, a novel member of the ACAD family, known as ACAD11, has been identified and shown to be highly expressed in the heart [11]. ACAD11 may function as a mitochondrial enzyme with long chain acyl-CoA activity in oligodendrocytes [11]. Notably, ACAD11 has been reported to be involved in the metabolism of hydroxylated fatty acid, which are important intermediates in lipid metabolism and signaling [12]. Therefore, regulating ACAD11 activity may reverse the pathological remodeling of DCM.

Protein ubiquitination is a multi-functional post-translational modification, with different polyubiquitin chains mediating various cellular processes [13]. The most common type is K48-linked polyubiquitination, which targets proteins for degradation, while K63-linked polyubiquitination is typically involved in non-degradation processes, including signal transduction, DNA repair, and cell survival [13]. Ubiquitin-specific protease 38 (USP38) is a member of deubiquitinating enzyme family that acts by removing different polyubiquitin chains from substrate proteins in various functional contexts. Our previous study demonstrated that USP38 aggravates pathological cardiac remodeling by removing K48-linked polyubiquitin chains of phospho-TANK-binding kinase 1 [14]. Moreover, USP38 has been reported to clean K63-linked polyubiquitin chains from histone deacetylases 1(HDAC1), thereby enhancing its deacetylase activity [15]. However, the mechanisms of USP38 in DCM is poorly understood.

In this study, we demonstrate that USP38 accelerates the progression of DCM and heart failure, increasing vulnerability to VAs. This effect is primarily driven by the decreased K63-linked polyubiquitination level of ACAD11, which triggers the mitochondrial dysfunction and pathological cardiac remodeling.

## 2. Methods

### 2.1. Detailed methods

Further information on experimental methods can be found in the Supplementary Material.

### 2.2. Animals and animal models

Cardiomyocyte-specific Usp38 transgenic mice (Usp38-TG), cardiomyocyte-specific Usp38 knockout mice ($Usp38^{cko}$), along with their respective control strains (NTG and $Usp38^{fl/fl}$), were constructed in Cyagen Biotechnology [16]. All procedures involving animals were conducted in accordance with the NIH guidelines for the Care and Use of Laboratory Animals and approved by the Animal Care and Use Committee of Renmin Hospital of Wuhan University (WDRM20230906). Male mice aged 8–10 weeks were selected for the experiment. Diabetes was induced by administrating intraperitoneal injections of streptozotocin (STZ, Sigma Aldrich, St, Louis, MO, USA) at dose of 50 mg/kg for 5 consecutive days. Control mice received citrate buffer (CB) injections for the same duration. One week following injections, mice with random blood glucose ≥16.7 mmol/L were considered diabetic and were selected for subsequent experiments. After additional 11 weeks of feeding, mice were deeply euthanized, and heart tissues were collected for analysis.

### 2.3. Statistical analysis

Data are presented as mean ± standard deviation. The normality of the data distribution was evaluated using the Shapiro-Wilk test. The Student's *t*-test was used to compare two groups, while one-way ANOVA followed by Tukey's post-hoc test was applied for comparisons among multiple groups. The Fisher's exact test was used to analyze induction rate of ventricular arrhythmias. Statistical analysis was performed using GraphPad Prism 9.0.0 software. For all statistical comparisons, a *P*-value of less than 0.05 was considered statistically significant.

## 3. Results

### 3.1. USP38 expression is upregulated in diabetic myocardium

To investigate the role of deubiquitinating enzymes in DCM, we first analyzed the GSE197850 and GSE202418 datasets from GEO database. The analysis revealed a significant upregulation of Usp38 mRNA in diabetic hearts (Fig. 1A–C). Meanwhile, the results of western blotting and immunofluorescence staining showed increased protein level of USP38 in diabetic hearts (Fig. 1D–G). Similarly, high glucose (HG) treatment of neonatal rat cardiomyocytes (NRCMs) also resulted in elevated in USP38 expression (Fig. 1H and I). In contrast, no significant changes were observed in neonatal rat cardiac fibroblasts (NRCFs) exposed to HG (Fig. 1J and K). Based on these results, USP38 was selected for further investigation in subsequent experiments.

### 3.2. Cardiomyocyte-specific USP38 overexpression accelerates cardiac electrical remodeling in diabetic mice

To determine the role of USP38 in diabetes-induced cardiac electrical remodeling, we constructed a Usp38-TG mouse line, with overexpression efficiency of USP38 verified by western blotting (Fig. S1A). Mice were intraperitoneally injected with or without streptozotocin (STZ), and experimental groups and timeline were depicted in Figure S1B. Surface electrocardiogram (ECG) analysis discovered prolonged QT interval and QTc interval in diabetic mice, which was further exacerbated in Usp38-TG diabetic mice (Fig. S1C–G). No significant differences were observed in the RR interval and QRS interval among groups (Fig. S1C–G). In vivo electrophysiological study demonstrated a prolonged action potential duration (APD) at 90 % repolarization (APD90) in diabetic mice, with greater prolongation observed in Usp38-TG diabetic mice (Fig. S2A and S2B). Similar results were observed in APD alternans (ALT) (Fig. S2C and S2D). Likewise, Usp38-TG diabetic mice exhibited increased vulnerability to ventricular arrhythmias (VAs), as demonstrated by higher induction rates (Fig. S2E and S2F). According to RNA-sequencing analysis on diabetic hearts of Usp38-TG mice and NTG mice, we identified 442 differently expressed genes (DEGs), visualized through heatmap and volcano plot (Fig. S3A and S3B). Notably, Usp38 mRNA level was extremely upregulated in Usp38-TG diabetic hearts than NTG diabetic hearts (Fig. S3B). Gene ontology (GO) analysis revealed significant enrichment in potassium ion transmembrane transporter activity (Fig. S3C). Therefore, we assessed the protein level of potassium ion channel by western blotting. Usp38-TG diabetic mice exhibited significantly reduced expression of Kv4.2 and Kv4.3, key components of transient outward potassium current ($I_{to}$) (Fig. S3D and S3E). These findings suggest that cardiomyocyte-specific USP38 overexpression accelerates diabetes-induced cardiac electrical remodeling.

### 3.3. Cardiomyocyte-specific USP38 overexpression aggravates cardiac dysfunction and cardiac structural remodeling in diabetic mice

To explore the role of USP38 on diabetic cardiac structural remodeling, we monitored physiological parameters such as blood glucose and body weight, with no significant differences observed between groups of diabetic mice (Fig. 2A–D). Echocardiographic assessment revealed

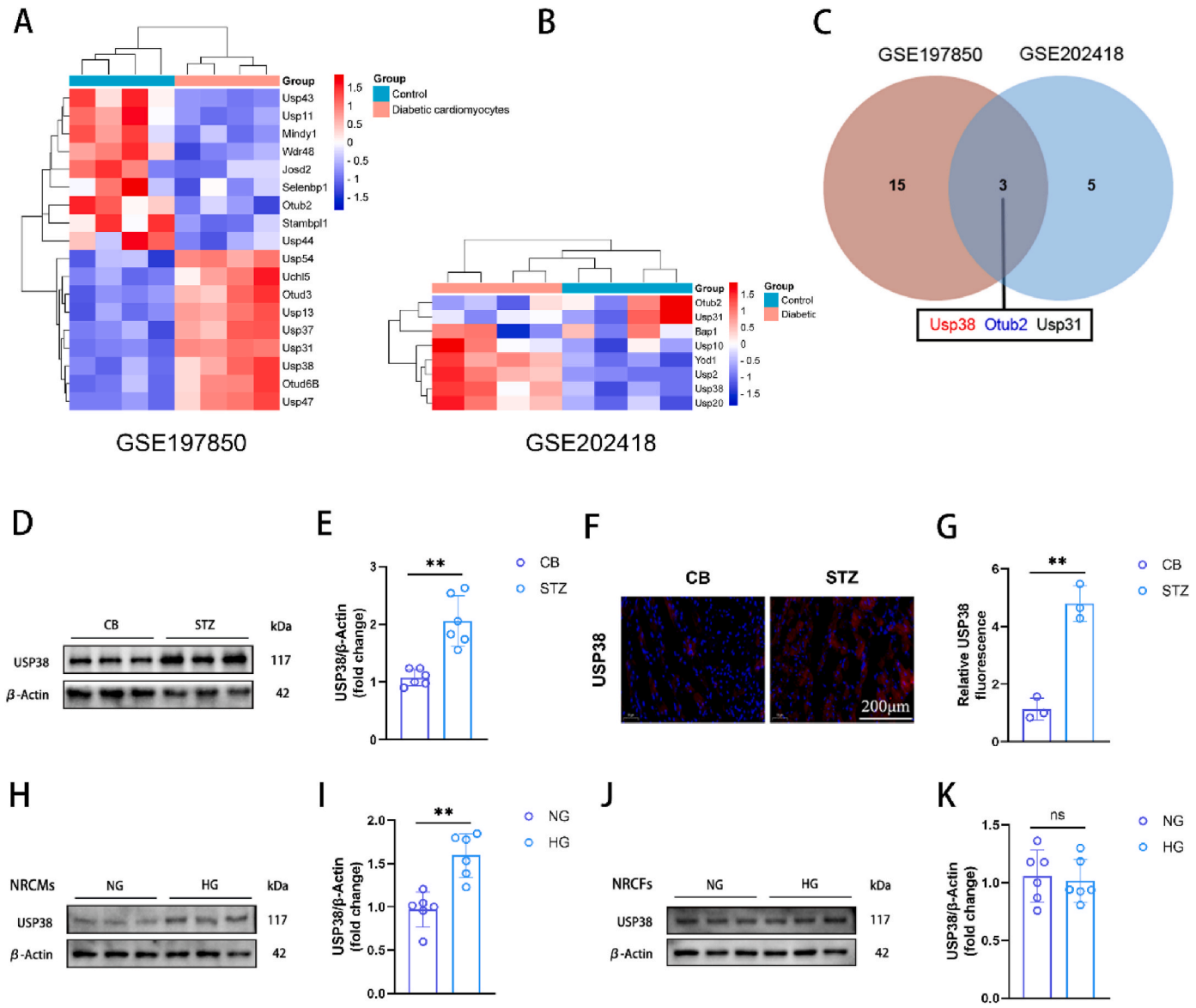


**Fig. 1.** The expression of USP38 is upregulated in diabetic myocardium.
**(A)** Heatmap of differentially expressed deubiquitinating enzyme genes in GSE197850. **(B)** Heatmap of differentially expressed deubiquitinating enzyme genes in GSE202418. **(C)** Venn diagram of differentially expressed deubiquitinating enzyme genes in GSE197850 and GSE202418. **(D–E)** Representative immunoblots and corresponding quantification showing cardiac USP38 in ventricular tissues (n = 6). **(F–G)** Representative images and corresponding quantification showing USP38 in ventricular tissues (magnification × 40) (n = 3). **(H–I)** Representative immunoblots and quantification showing USP38 in NRCMs (n = 6). **(J–K)** Representative immunoblots and corresponding quantification showing USP38 in NRCFs (n = 6). Data was calculated by student's *t*-test (unpaired, two-tailed, two groups). $^{*}P < 0.05$, $^{**}P < 0.01$.

impaired cardiac systolic and diastolic function in diabetic mice, characterized by lower left ventricular ejection fraction and shortening fraction (LVEF and LVFS), and higher left ventricle internal dimension at end-systole and at end-diastole (LVIDs and LVIDd). These impairments were further exacerbated in Usp38-TG diabetic mice (decreased LVEF and LVFS, and increased LVIDs) (Fig. 2E–I). Similarly, Usp38-TG diabetic mice exhibited prominent cardiac diastolic dysfunction, as demonstrated by a reduction of early to late diastolic transmitral flow velocity (E/A ratio) (Fig. 2J).

We next performed morphological analysis of cardiac tissues. H&E staining revealed myocardial disarray in NTG diabetic mice, which was further exacerbated in Usp38-TG diabetic mice (Fig. 2K). Masson's staining showed increased collagen deposition in Usp38-TG diabetic mice (Fig. 2K and L). Likewise, immunohistochemical staining confirmed elevated expression of collagen I and collagen III in Usp38-TG diabetic hearts (Fig. 2M–O), and western blotting further supported these findings, showing increased Collagen I, Collagen III, and TGF-β expression in Usp38-TG diabetic hearts (Fig. 2P and Q).

Moreover, inflammation and apoptosis are hallmarks of DCM. As shown in Fig. 3A and B, western blotting analysis revealed elevated levels of TNF-α, IL-1β, and IL-6 in diabetic hearts, with further elevation observed in Usp38-TG diabetic mice. TUNEL staining analysis showed increased cardiomyocyte apoptosis in Usp38-TG diabetic hearts (Fig. 3C and D). Additionally, western blotting analysis showed higher expression of Bax and lower expression of Bcl-2 in Usp38-TG diabetic hearts than NTG diabetic hearts (Fig. 3E and F). Collectively, these data suggest that cardiomyocyte-specific USP38 overexpression aggravates cardiac dysfunction and structural remodeling in diabetic mice.

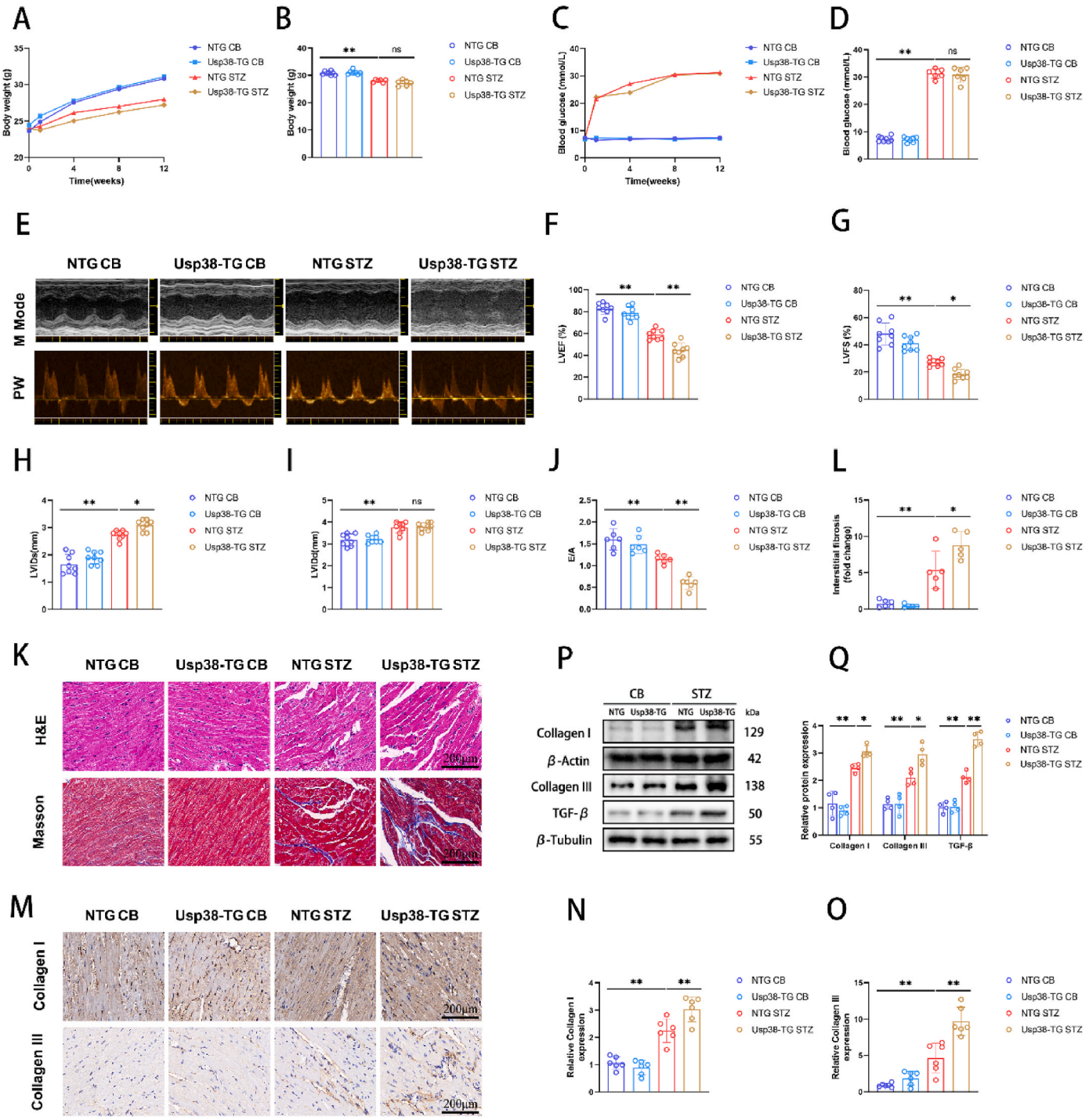


**Fig. 2.** Cardiomyocyte-specific USP38 overexpression aggravates cardiac dysfunction and cardiac structural remodeling in diabetic mice.
**(A)** Change in body weight in each group after 0w, 1w, 4w, 8w and 12w (n = 6–7). **(B)** Statistical analysis of body weight in each group after 12 w (n = 6–7). **(C)** Change in blood glucose in each group after 0w, 1w, 4w, 8w and 12w (n = 6–7). **(D)** Statistical analysis of blood glucose in each group after 12 w (n = 6–7). **(E–J)** Representative images and corresponding quantification for echocardiography(n = 6–7). **(K–L)** Representative images of H&E stained and Masson stained, and corresponding quantification based on myocardial fibrosis (magnification × 40) (n = 6). **(M–O)** Representative immunohistochemical images and corresponding quantification of Collagen I and Collagen III (magnification × 40) (n = 6). **(P–Q)** Representative immunoblots and corresponding quantification for Collagen I, Collagen III and TGF-β (n = 4). Data was calculated by one-way analysis of variance (Tukey's multiple comparisons test). $^{*}P < 0.05$, $^{**}P < 0.01$.

### *3.4. Cardiomyocyte-specific USP38 overexpression disturbs fatty acid oxidation and aggravates mitochondrial dysfunction in diabetic mice*

To further elucidate the underlying molecular mechanism of USP38's effects, we conducted RNA-sequencing analysis on diabetic hearts of Usp38-TG mice and NTG mice. Gene ontology (GO) analysis of DEGs revealed enrichment in fatty acid oxidation (Fig. 4A). Based on these findings, we evaluated lipid contents and mitochondrial morphology in myocardial tissues. Interestingly, no significant lipid deposition was observed in the hearts of the different groups by Oil Red O staining (Fig. 4B). However, transmission electron microscope showed abnormal mitochondrial morphology and lipid droplets in diabetic

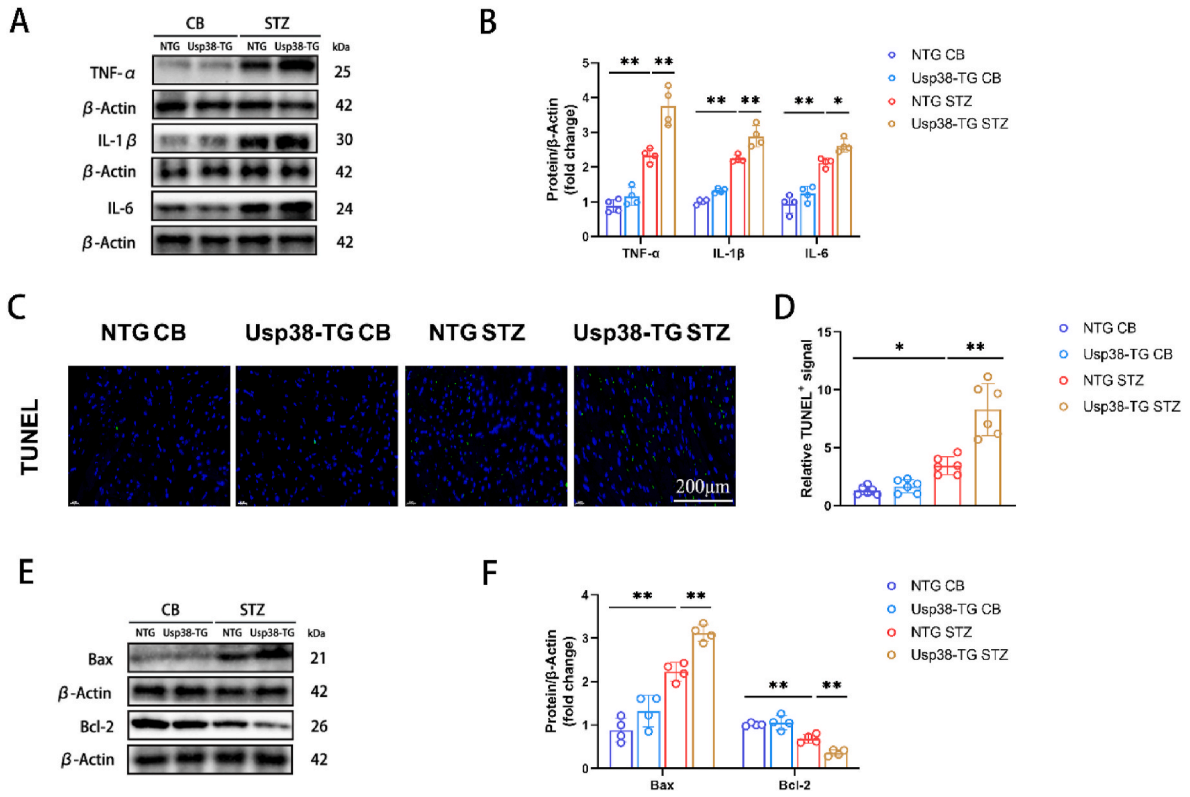


**Fig. 3.** Cardiomyocyte-specific USP38 overexpression aggravates cardiac inflammation and cardiomyocytes apoptosis in diabetic mice.
**(A–B)** Representative immunoblots and corresponding quantification for TNF-α, IL-1-β and IL-6 (n = 4). **(C–D)** Representative images and corresponding quantification for TUNEL staining (magnification × 40) (n = 6). **(E–F)** Representative immunoblots and corresponding quantification for Bax and Bcl-2 (n = 4). Data was calculated by one-way analysis of variance (Tukey's multiple comparisons test). $^{*}P < 0.05$, $^{**}P < 0.01$.

myocardial tissues (Fig. 4C and D). Compared to NTG diabetic mice, we observed more pronounced mitochondrial damage in Usp38-TG diabetic myocardial tissues, including the loss and swelling of mitochondrial cristae (Fig. 4C). We then analyzed the expression of gene related to mitochondrial fusion and fission by RT-qPCR. Mitochondrial fusion-related genes, such as Mfn2 and Opa1, were reduced in diabetic hearts, with further reduction observed in Usp38-TG diabetic mice (Fig. 4E). However, mitochondrial fission-related genes, including Drp1 and Fis1, did not show significant changes among groups (Fig. 4F). Mitochondrial dysfunction is often accompanied with lipid peroxidation and ROS production. Therefore, we detected lipid peroxidation using 4-hydroxynonenal (4-HNE) and reactive oxygen species (ROS) levels using dihydroethidium (DHE) assay. NTG diabetic mice exhibited enhanced lipid peroxidation and ROS accumulation, which was further aggravated in Usp38-TG diabetic mice (Fig. S4A–D). Additionally, the expression of anti-oxidant components, such as nuclear factor erythroid 2-related factor 2 (Nrf2) and heme oxygenase (HO-1), was significantly suppressed in Usp38-TG diabetic mice (Fig. S4E and S4F).

To further identify the role of USP38 overexpression in mitochondria dysfunction in vitro, we transfected NRCMs with adenovirus carrying Usp38 (AdUsp38) or null transfection (AdGFP) and treated them with normal glucose (NG) or HG. We first assessed mitochondria morphology and found that HG treatment caused fragmented and swollen mitochondria in NRCMs. The defect was more severe in NRCMs with overexpressing USP38 under HG conditions (Fig. 4G and H). Second, we measured mitochondrial ROS production, which was increased in HG-treated NRCMs, and further elevated by USP38 overexpression (Fig. 4I and J). Consistent with in vivo results, the expression of anti-oxidant components, including Nrf2 and HO-1, was significantly down-regulated in HG-treated NRCMs with USP38 overexpression (Fig. S4G and S4H). Given that mitochondria are crucial for cellular energy production, we next evaluated mitochondrial membrane potential and ATP production. TMRE staining revealed that HG treatment reduced mitochondrial membrane potential in NRCMs, with USP38 overexpression further exacerbating this reduction (Fig. 4K and L). Then, we detected the ATP production and found that USP38 overexpression further reduced ATP content in NRCMs treated with HG (Fig. 4M). Collectively, these results indicate that USP38 overexpression disrupts fatty acid oxidation and exacerbates mitochondrial dysfunction in diabetic conditions.

### 3.5. *Cardiomyocyte-specific USP38 deficiency ameliorates cardiac remodeling and mitochondrial dysfunction in diabetic mice*

To further explore the function of USP38 in DCM, we generated $Usp38^{cko}$ mice, with knockout efficiency of USP38 verified by western blotting (Fig. S5A). The experimental group and timeline were depicted in Figure S5B. Diabetes contributes to electrical instability, which can lead to VAs and sudden cardiac death. $Usp38^{cko}$ diabetic mice exhibited increased cardiac electrical stability, as evidenced by shortened QT interval and QTc interval (Fig. S5C–G), reduced APD90 and ALT, and decreased VAs induction rates (Fig. S6A–E). The expression of Kv4.2 and Kv4.3 also was upregulated in $Usp38^{cko}$ diabetic mice than $Usp38^{fl/fl}$ diabetic mice (Fig. S6F).

In line with Usp38-TG diabetic mice, there were no significant differences in blood glucose levels and body weight between groups of diabetic mice (Fig. 5A–D). Echocardiography revealed improved cardiac function in $Usp38^{cko}$ diabetic mice, including higher LVEF, LVFS and E/A ratio, as well as lower LVIDs (Fig. 5E–J). Additionally, $Usp38^{cko}$ diabetic mice exhibited reduced myocardial fibrosis and collagen expression (Fig. 5K–N). We next assessed the expression of inflammatory and apoptotic markers. Compared with $Usp38^{fl/fl}$ diabetic mice, $Usp38^{cko}$ diabetic mice showed lower expression of TNF-α, IL-1β, IL-6, and Bax, and higher expression of Bcl-2 in myocardial tissues (Fig. 5O–R).

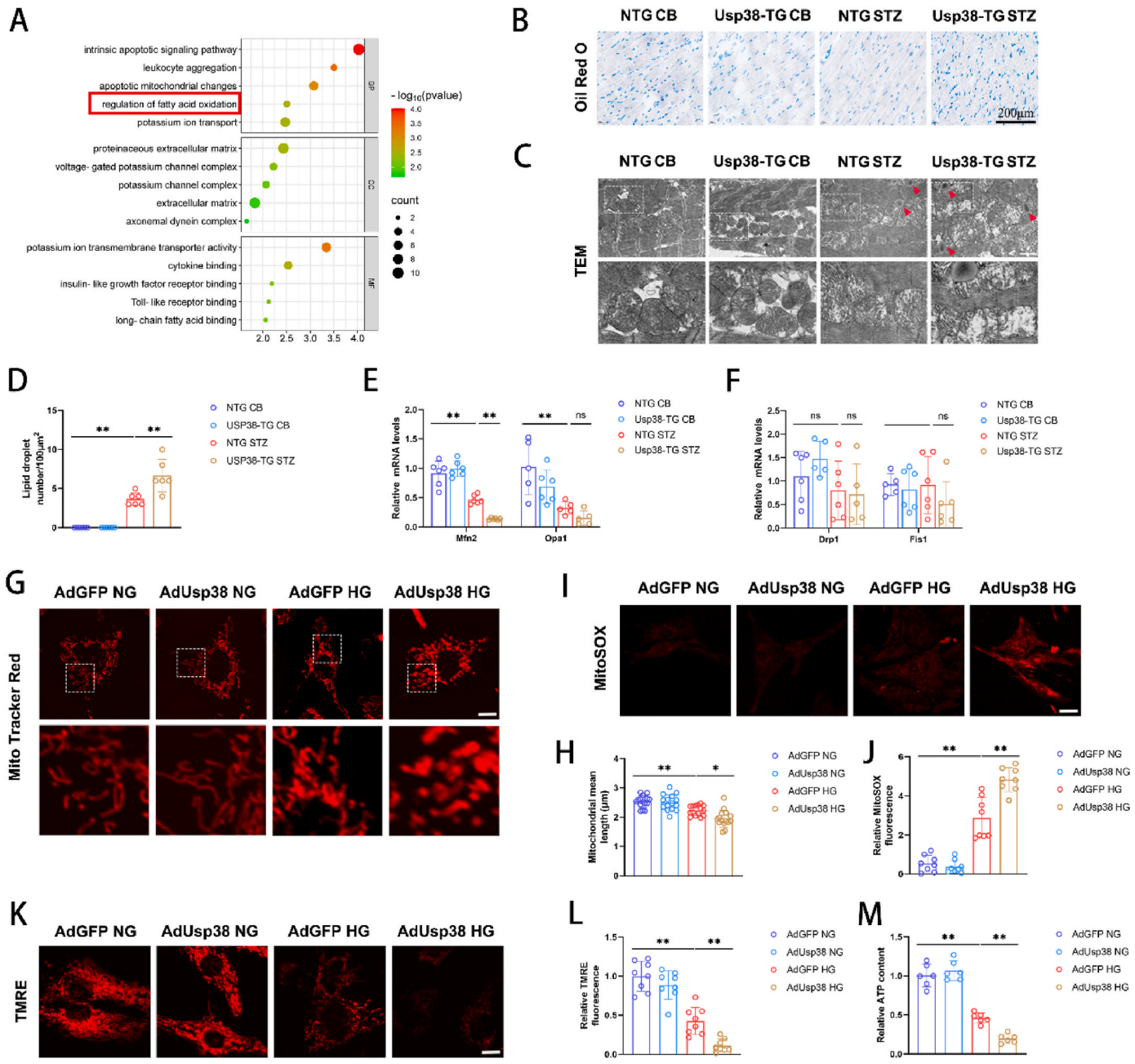


**Fig. 4.** Cardiomyocyte-specific USP38 overexpression disturbs fatty acid oxidation and aggravates mitochondrial dysfunction.
**(A)** Gene ontology (GO) analysis of DEGs between Usp38-TG STZ group and NTG STZ group. **(B)** Representative images of Oil Red O staining (magnification × 40) (n = 6). **(C–D)** Representative images and corresponding quantification for transmission electron microscope based on lipid droplet numbers/100 μm$^2$ (n = 6). (top, magnification × 15000, scale bar = 10 μm). **(E–F) mRNA level** of Mfn2, Opa1, Drp1 and Fis1 (n = 5–6). **(G–H)** Representative images and corresponding quantification for Mito Tracker staining in NRCMs (n = 15), (top, magnification × 1200, scale bar = 10 μm). **(I–J)** Representative images and corresponding quantification for MitoSOX staining in NRCMs (n = 8), (magnification × 600, scale bar = 20 μm). **(K–L)** Representative images and corresponding quantification for TMRE staining in NRCMs (n = 8), (magnification × 1200, scale bar = 10 μm). **(M)** ATP content in NRCMs (n = 5–6). Data was calculated by one-way analysis of variance (Tukey's multiple comparisons test). *$P < 0.05$, **$P < 0.01$.

Mitochondrial fusion-related genes (Mfn2 and Opa1) were upregulated in Usp38$^{cko}$ diabetic hearts (Fig. S7A), while mitochondrial fission-related genes (Drp1 and Fis1) remained unchanged (Fig. S7B). In addition, Usp38$^{cko}$ diabetic mice exhibited increased expression of HO-1 and Nrf2 (Fig. S7C and S7D).

In vitro experiments, NRCMs were transfected with adenovirus short hairpin Usp38 (AdshUsp38) or null transfection (AdshRNA) and treated with NG or HG. We discovered that NRCMs with USP38 knockdown exhibited improved mitochondrial morphology based on mitochondrial length and fragment under HG conditions (Fig. 6A and B). Additionally, we found that USP38 knockdown reduced mitochondrial ROS production in HG-treated NRCMs (Fig. 6C and D). Likewise, USP38 knockdown increased the anti-oxidant capacity of HG-treated NRCMs by promoting HO-1 and Nrf2 expression (Fig. S7E and S7F). Next, we explored the effect of USP38 knockdown on energy metabolism of HG-treated NRCMs. NRCMs with USP38 knockdown exhibited increased mitochondrial membrane potential (Fig. 6E and F) and higher ATP production (Fig. 6G) under HG conditions. Together, these data indicate that USP38 deficiency improves diabetes-induced mitochondrial dysfunction and cardiac remodeling.

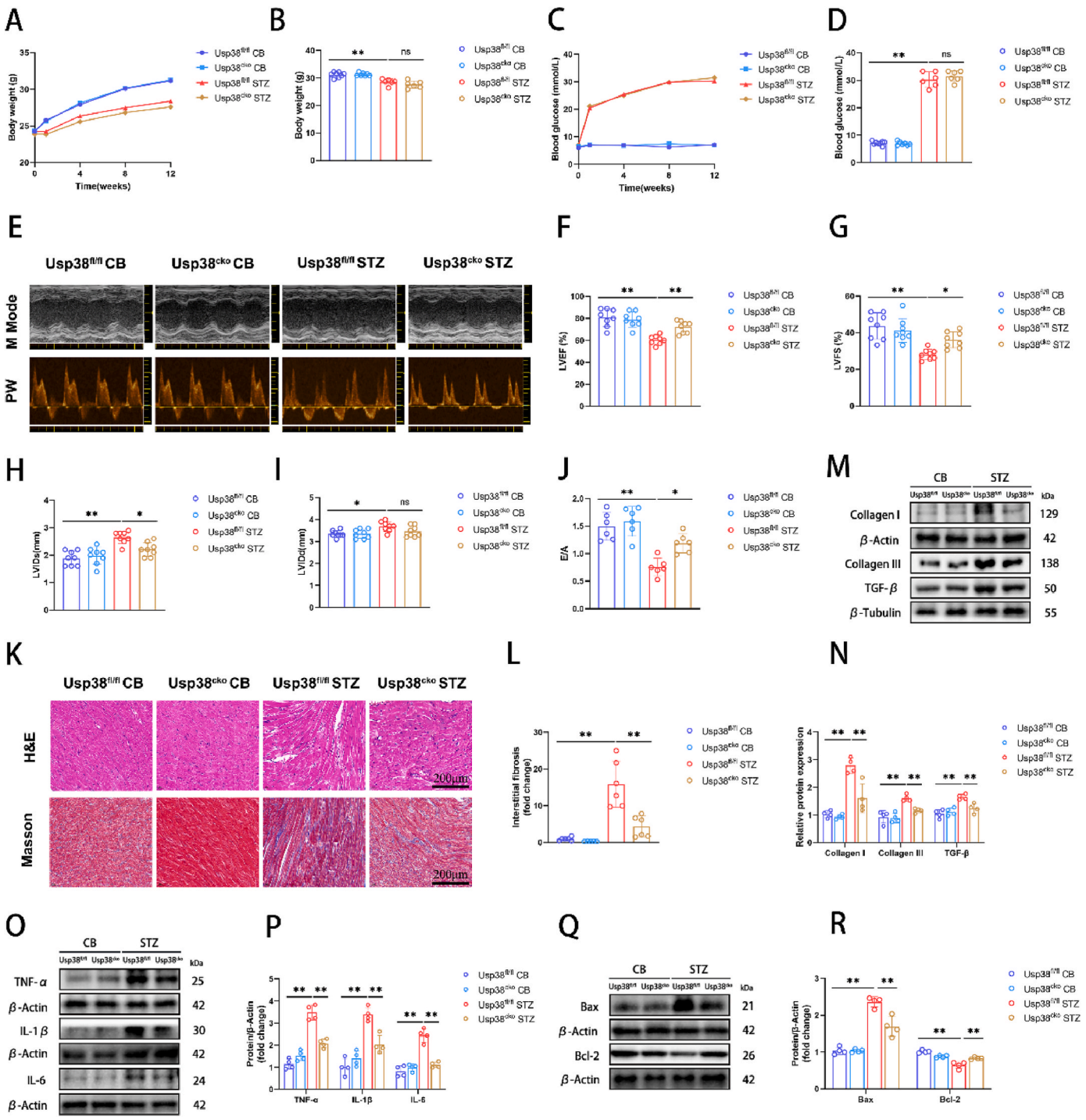


**Fig. 5.** Cardiomyocyte-specific USP38 deficiency improves cardiac function and cardiac structural remodeling in diabetic mice.
**(A)** Change in body weight in each group after 0w, 1w, 4w, 8w and 12w (n = 6–7). **(B)** Statistical analysis of body weight in each group after 12 w (n = 6–7). **(C)** Change in blood glucose in each group after 0w, 1w, 4w, 8w and 12w (n = 6–7). **(D)** Statistical analysis of blood glucose in each group after 12 w (n = 6–7). **(E–J)** Representative images and corresponding quantification for echocardiography (n = 6–7). **(K–L)** Representative images of H&E stained and Masson stained, and corresponding quantification based on myocardial fibrosis (magnification × 40) (n = 6). **(M–N)** Representative immunoblots and corresponding quantification for Collagen I, Collagen III and TGF-β (n = 4). **(O–P)** Representative immunoblots and corresponding quantification for TNF-α, IL-1-β and IL-6 (n = 4). **(Q–R)** Representative immunoblots and corresponding quantification for Bax and Bcl-2 (n = 4). Data was calculated by one-way analysis of variance (Tukey's multiple comparisons test). $^{*}P < 0.05$, $^{**}P < 0.01$.

### 3.6. USP38 interacts with ACAD11 to modulate ACAD11 activity

To investigate potential USP38-binding partners, we performed immunoprecipitation and mass spectrometry (IP-MS) analysis. The experimental workflow is shown in Fig. 7A. A total of 1066 protein candidates were obtained from the USP38-binding protein complex **(Excel file S)**, with ACAD11 emerging as the top candidate (Fig. 7B and C). Based on these findings, we performed Co-immunoprecipitation (Co-IP) to confirm the interaction between USP38 and ACAD11. As expected, the endogenous binding of USP38 and ACAD11 was confirmed in

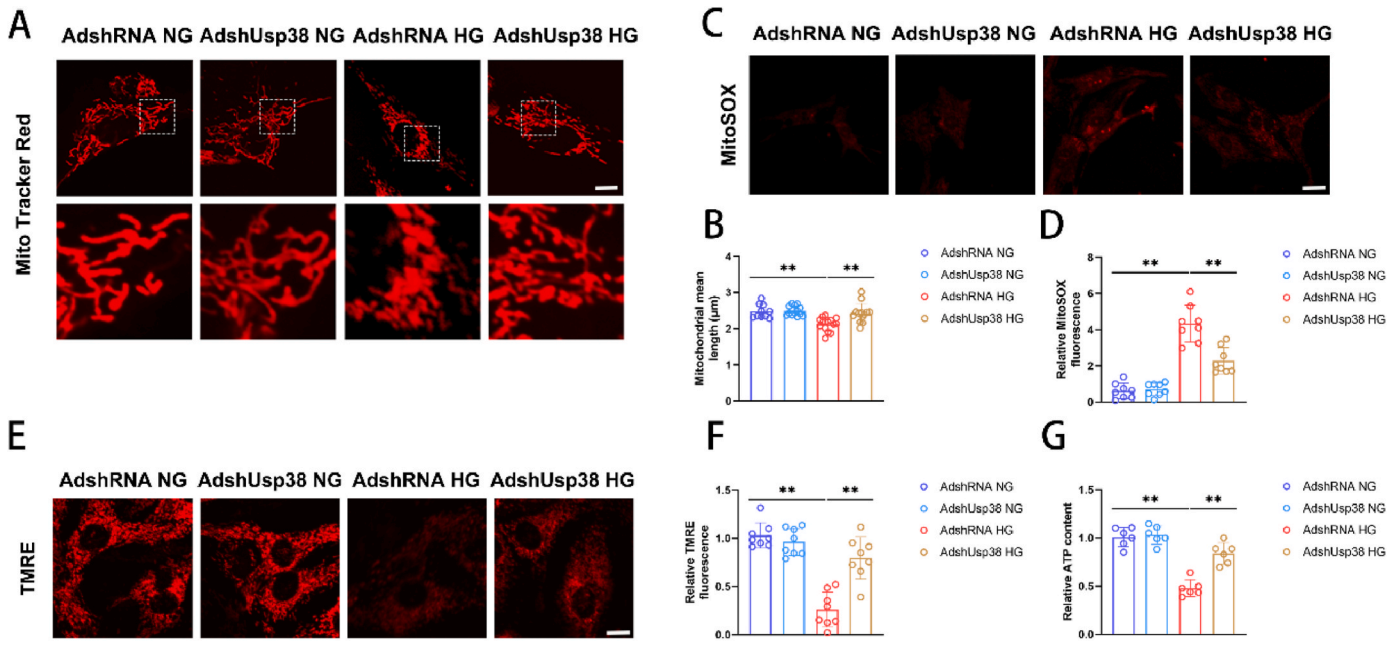


**Fig. 6.** USP38 downregulation improves mitochondrial function in HG-treated NRCMs.
**(A–B)** Representative images and corresponding quantification for Mito Tracker staining (n = 10–15). (top, magnification × 1200, scale bar = 10 μm). **(C–D)** Representative images and corresponding quantification for MitoSOX staining (n = 8), (magnification × 600, scale bar = 20 μm). **(E–F)** Representative images and corresponding quantification for TMRE staining (n = 8). (magnification × 1200, scale bar = 10 μm). **(G)** ATP content in NRCM (n = 5–6). Data was calculated by one-way analysis of variance (Tukey's multiple comparisons test). $^{*}P < 0.05$, $^{**}P < 0.01$.

NRCMs with antibodies against USP38 and ACAD11 (Fig. 7D and E). Likewise, the exogenous binding of USP38 and ACAD11 was verified in HEK293T cells transfected with plasmid encoding USP38 and ACAD11 (Fig. 7F and G). Immunofluorescence staining further confirmed the co-location of USP38 and ACAD11 in NRCMs (Fig. 7H). Recent study has reported that ACAD11 is located to peroxisomes and participates in the oxidation of 4-hydroxy fatty acid [12]. Therefore, we detected the subcellular location of ACAD11 and found it is present in both mitochondria and peroxisomes (Fig. 7I and J). To further determine the binding domains of USP38 and ACAD11, we constructed the two truncations of USP38 and four truncations of ACAD11. Our results showed that USP38 failed to bind to ACAD11 with the absence of the APH domain (ΔAPH), and ACAD11 failed to bind to USP38 with the absence of the C domain (ΔC). These findings indicate that the C domain of USP38 interacts with the APH domain of ACAD11 (Fig. 7K–N).

Considering the deubiquitinating function of USP38, we next evaluated its effect on the post-translational modification of ACAD11. As expected, USP38 overexpression reduced the ubiquitination level of ACAD11, whereas the effect disappeared under USP38 mutant conditions (Fig. 8A). We further investigated the specific polyubiquitination modifications. The results revealed that USP38 specifically blocked K63-linked polyubiquitination of ACAD11, but not K48-linked polyubiquitination in HEK293T cells (Fig. 8B). Likewise, we observed that USP38 overexpression reduced K63-linked polyubiquitination of ACAD11 in NRCMs under HG conditions (Fig. 8C). In contrast, USP38 knockdown increased K63-linked polyubiquitination of ACAD11 in HG-treated NRCMs (Fig. 8D). Taken together, these findings indicate that USP38 specifically interacts with ACAD11 to reduce its K63-linked polyubiquitination.

### 3.7. USP38 regulates cardiac remodeling by promoting RAGE signaling pathway in diabetic mice

To explore the role of USP38 on lipid metabolism in diabetic mice, we performed lipidomic analysis on the heart of NTG diabetic mice and Usp38-TG diabetic mice. Differently lipid metabolites, such as cardiolipins, diacylglycerols and triglycerides, are shown in a bilateral bar diagram (Fig. 9A). Kyoto Encyclopedia of Genes and Genomes (KEGG) analysis of these differently lipid metabolites revealed enrichment in the AGE-RAGE signaling pathway in diabetic complications (Fig. 9B). Notably, KEGG analysis of DEGs also confirmed enrichment in AGE-RAGE signaling pathway in diabetic complications (Fig. 9C).

Therefore, we next assessed the expression of RAGE in diabetic hearts by immunofluorescence staining and western blotting. As expected, Usp38-TG mice exhibited increased expression of RAGE in diabetic hearts (Fig. 9D–G). Conversely, Usp38$^{cko}$ mice exhibited reduced expression of RAGE in diabetic hearts (Fig. 9H and I). Consistent results were found in HG-treated NRCMs (Fig. 9J–M). These results indicate that USP38 promotes RAGE signaling pathway in diabetic myocardium.

### 3.8. Inhibition of RAGE by FPS-ZM1 improves pathological cardiac remodeling in Usp38-TG diabetic mice

To further investigate whether USP38 promotes the progression of DCM through the RAGE pathway, we treated Usp38-TG diabetic mice with FPS-ZM1, a specific RAGE inhibitor, and the experimental timeline was depicted in Figure S8A. FPS-ZM1 increased cardiac electrical stability in Usp38-TG diabetic mice, manifested by shortened QT interval and QTc interval, and reduced induction rate of VAs (Fig. S8B–F). No significant differences in blood glucose and body weight were observed between Usp38-TG diabetic mice with or without FPS-ZM1 administration (Fig. 10A–D). Echocardiographic analysis showed improved cardiac function after FPS-ZM1 administration, as evidenced by increased LVEF, LVFS and E/A ratio (Fig. 10E–H). There results indicate that FPS-ZM1 significantly attenuates cardiac systolic and diastolic dysfunction in Usp38-TG diabetic mice. We subsequently assessed the effects of FPS-ZM1 on diabetes-induced cardiac structural remodeling. FPS-ZM1 alleviated myocardial disarray and myocardial fibrosis in Usp38-TG diabetic mice (Fig. 10I–N), suggesting that FPS-ZM1 alleviates cardiac structural remodeling in diabetes. In addition, FPS-ZM1 markedly reduced the expression of inflammatory marker in Usp38-TG diabetic mice (Fig. 10O and P). Collectively, these results indicate that

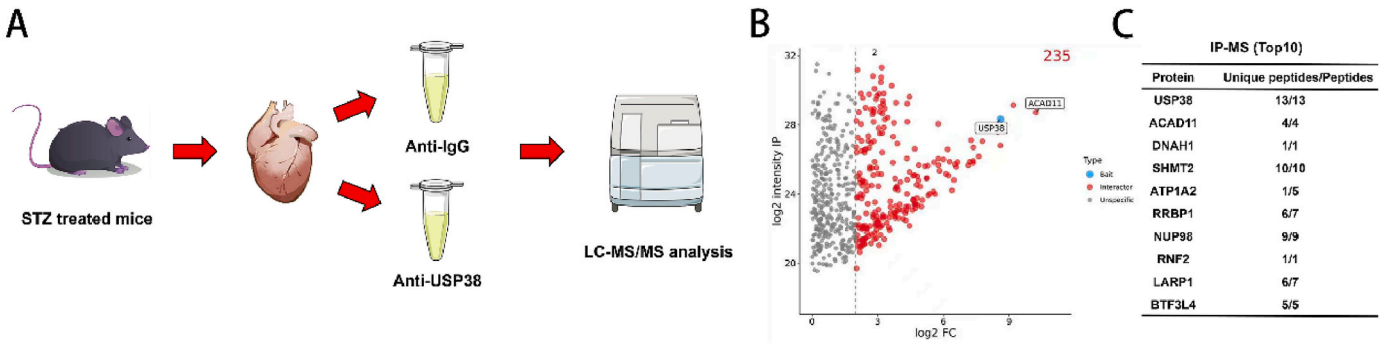


C

IP-MS (Top10)

| Protein | Unique peptides/Peptides |
|---|---|
| USP38 | 13/13 |
| ACAD11 | 4/4 |
| DNAH1 | 1/1 |
| SHMT2 | 10/10 |
| ATP1A2 | 1/5 |
| RRBP1 | 6/7 |
| NUP98 | 9/9 |
| RNF2 | 1/1 |
| LARP1 | 6/7 |
| BTF3L4 | 5/5 |

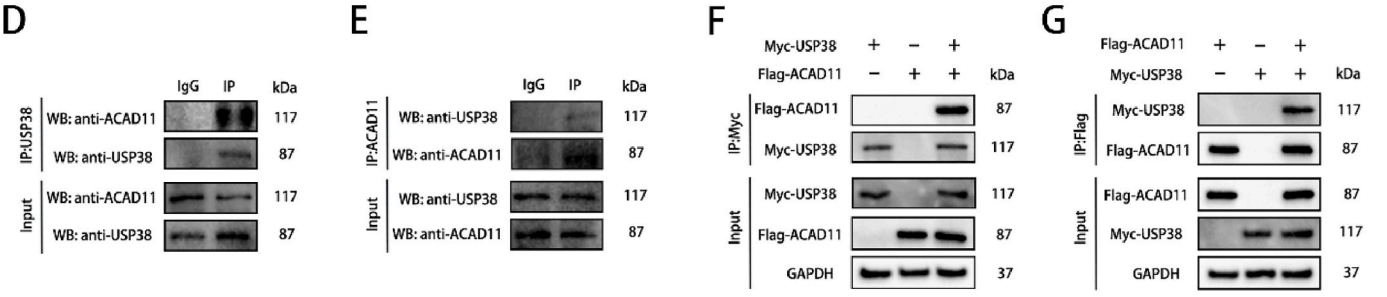


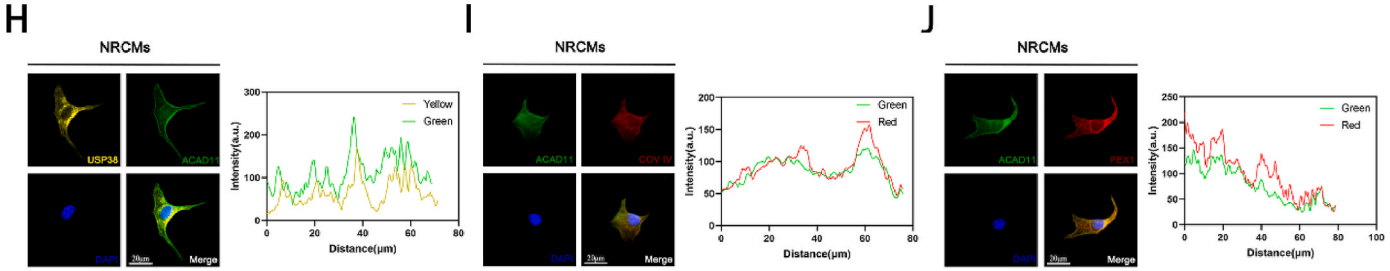


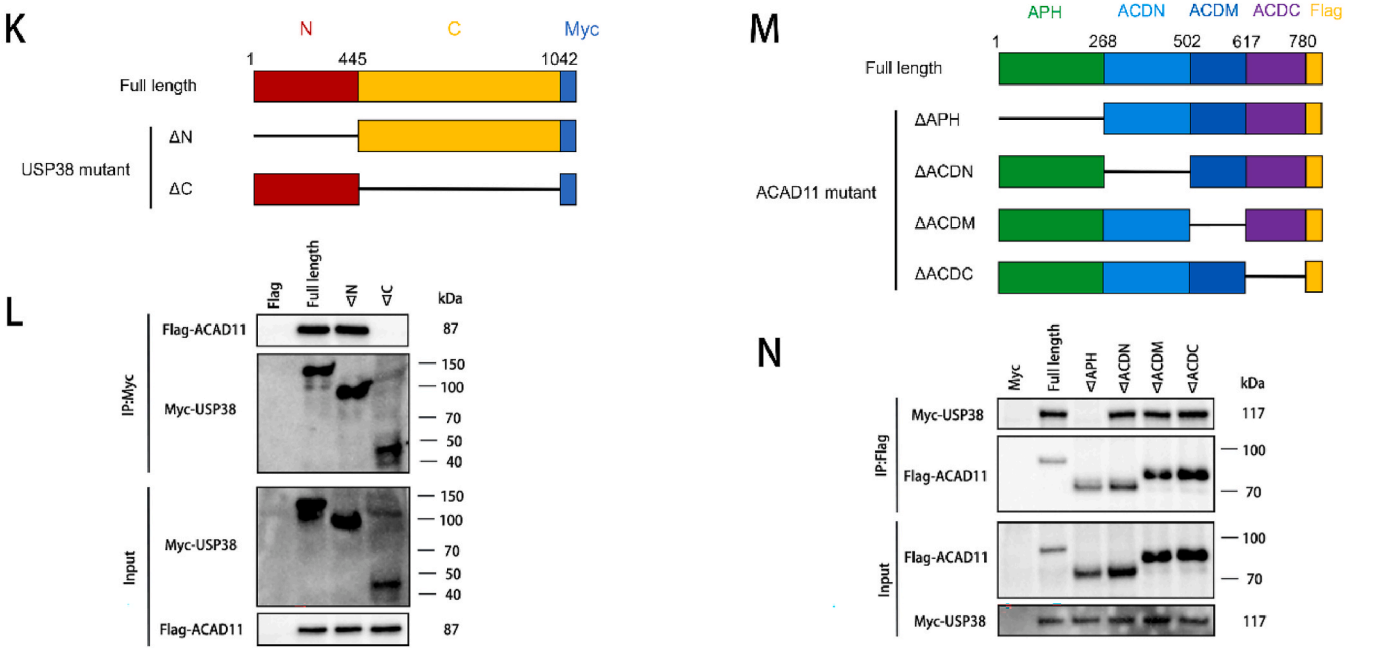


*(caption on next page)*

**Fig. 7.** USP38 interacts with ACAD11.
**(A–C)** The diagram of immunoprecipitation-mass spectrometry (IP-MS), and USP38-interacting Top 10 proteins. **(D–E)** Immunoblot showing the endogenous interaction between USP38 and ACAD11 in NRCMs. **(F–G)** Immunoblot showing the exogenous interaction between USP38 and ACAD11 in HEK293T cells. Cell lysates were extracted and immunoprecipitated with anti-Myc or anti-Flag antibody, followed by the detection of Flag-tag or Myc-tag. **(H)** Representative images of immunofluorescence staining for USP38 (yellow) and ACAD11 (green) in NRCMs. (magnification × 1200, scale bar = 20 μm). **(I)** Representative images of immunofluorescence staining for ACAD11 (green) and COV IV (red) in NRCMs. (magnification × 1200, scale bar = 20 μm). **(J)** Representative images of immunofluorescence staining for ACAD11 (green) and PEX1 (red) in NRCMs. (magnification × 1200, scale bar = 20 μm). **(K)** Schematic diagram showing the constructs expressing full-length USP38 or its truncated fragments. **(L)** Myc-tagged full-length or truncated USP38 were co-transfected with Flag-tagged full-length ACAD11 into HEK293T cells, respectively. Cell lysates were immunoprecipitated with anti-Myc antibody, and immunoblotting was performed using anti-Flag antibody. **(M)** Schematic diagram showing the constructs expressing full-length ACAD11 or its truncated fragments. **(N)** Flag-tagged full-length or truncated ACAD11 were co-transfected with Myc-tagged full-length USP38 into HEK293T cells, respectively. Cell lysates were immunoprecipitated with anti-Flag antibody, and immunoblotting was performed using anti-Myc antibody.

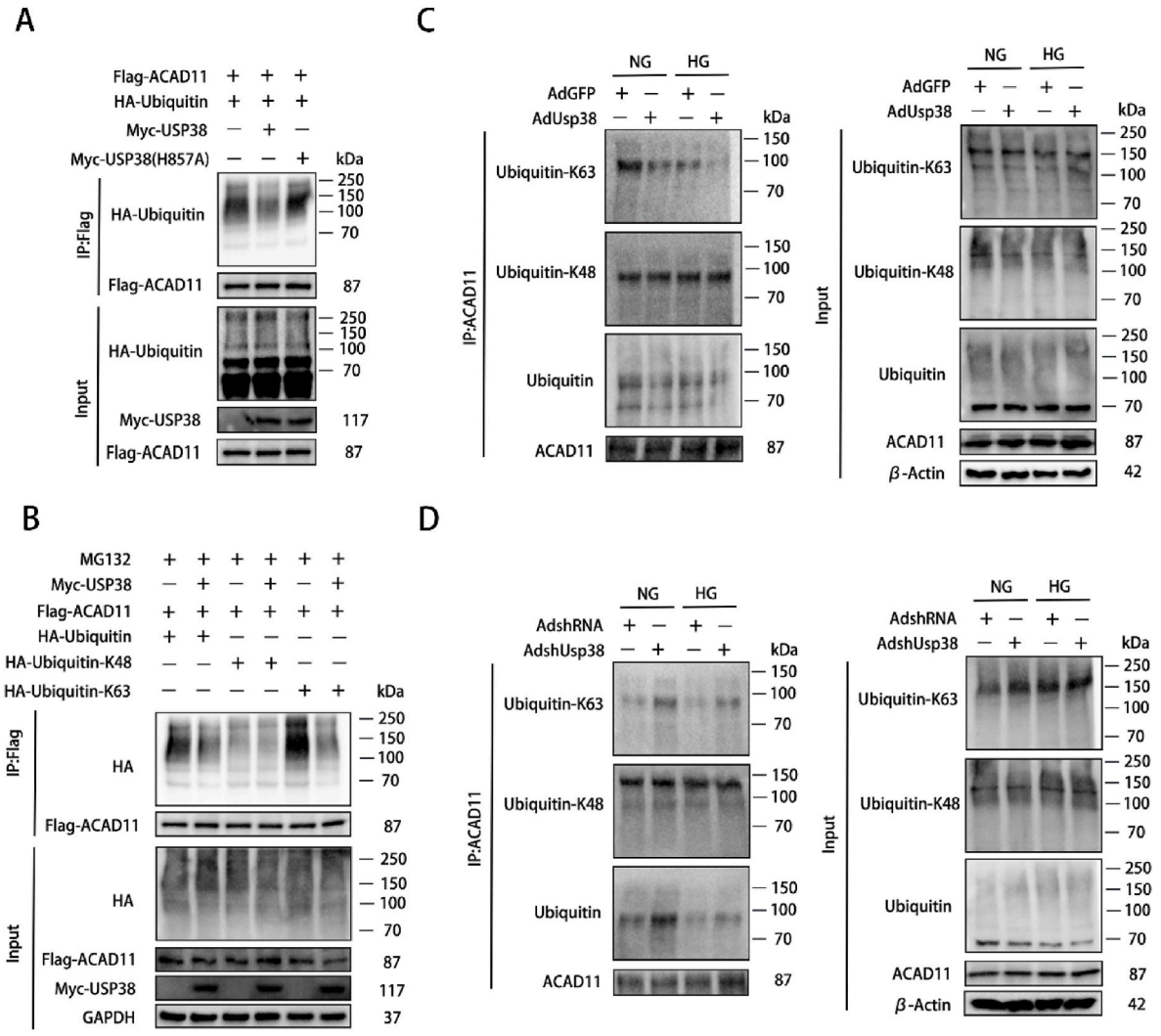


**Fig. 8.** USP38 removes the K63-linked polyubiquitination of ACAD11.
**(A)** Ubiquitination assay of ACAD11 in HEK293T cells transfected with Myc-tagged USP38 or catalytically inactive mutant USP38H857A. **(B)** Ubiquitination assay of ACAD11 in HEK293T cells transfected with HA-tagged ubiquitin-K63, HA-tagged ubiquitin-K48, HA-tagged ubiquitin, Myc-tagged USP38 and Flag-tagged ACAD11. **(C–D)** Ubiquitination assay of ACAD11 in NRCMs.

FPS-ZM1 effectively mitigates the detrimental effects induced by USP38 overexpression in diabetic hearts.

## 4. Discussion

Patients with diabetes are at high risk for developing heart failure and ventricular arrhythmia [2,3,5,17]. The molecular mechanism underlying DCM are complex and have attracted considerable attention over the past few decades. In this study, we uncover that cardiomyocyte-specific USP38 overexpression in diabetic hearts disturbs lipid metabolism and mitochondrial function, activates the RAGE signaling pathway, and leads to cardiac inflammation, myocardial fibrosis, cardiomyocyte apoptosis, and ventricular electrical instability. Conversely, loss of USP38 function in diabetic hearts improves cardiac remodeling and reduces vulnerability to VAs. Mechanistically, USP38 directly interacts with ACAD11 and deubiquitinates it, resulting in abnormal fatty acid oxidation. Our findings reveal a novel pathogenesis for DCM and suggest that targeting the USP38-ACAD11 axis may

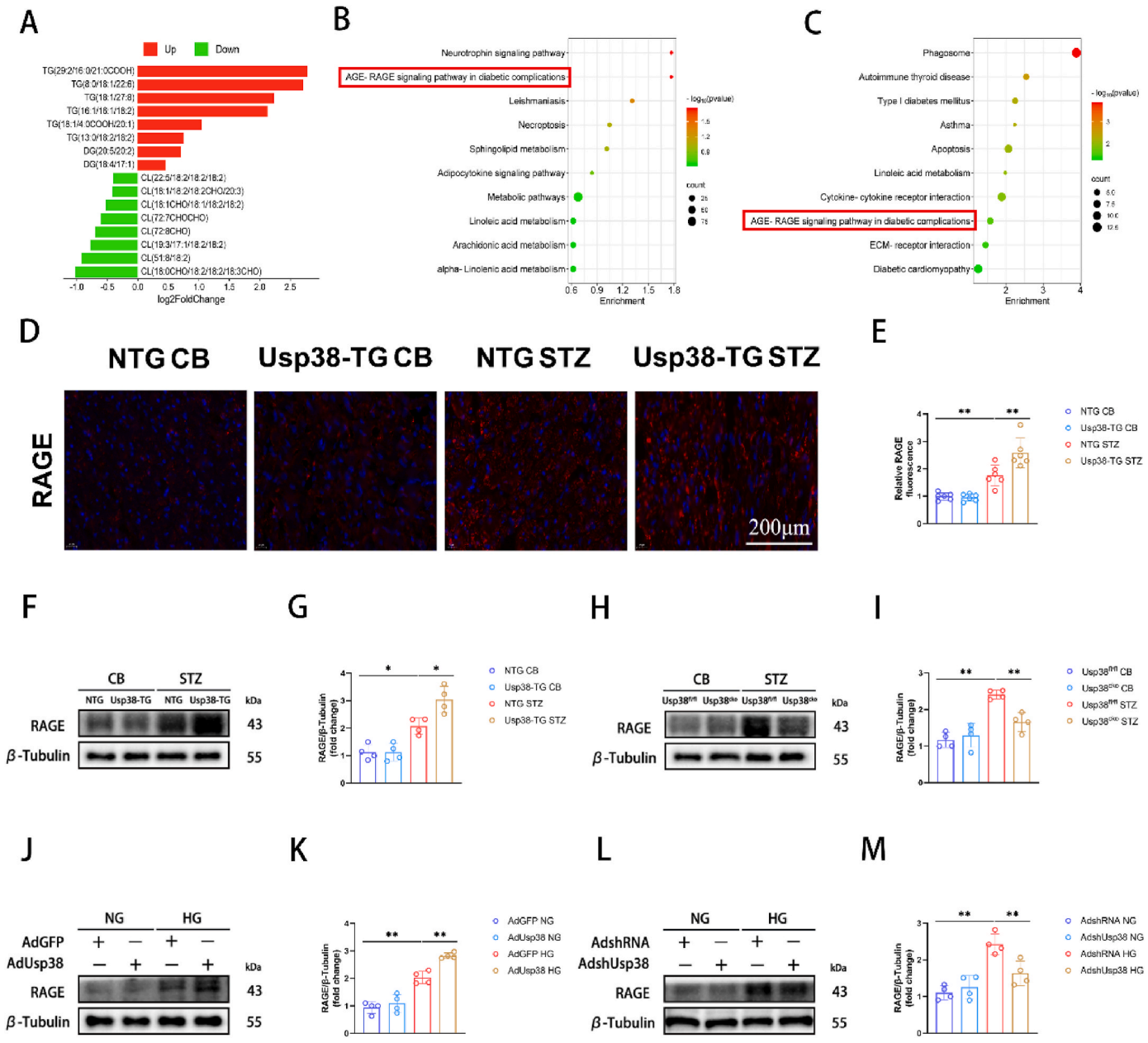


**Fig. 9.** USP38 regulates cardiac remodeling by promoting RAGE signaling pathway in diabetic mice.
**(A)** Bilateral bar diagram of differently lipid metabolites between Usp38-TG STZ group and NTG STZ group. **(B)** Kyoto Encyclopedia of Genes and Genomes (KEGG) analysis of differently lipid metabolites between Usp38-TG STZ group and NTG STZ group. **(C)** KEGG analysis of DUBs between Usp38-TG STZ group and NTG STZ group. **(D–E)** Representative immunofluorescence staining images and corresponding quantification of RAGE (magnification × 40) (n = 4). **(F–I)** Representative immunoblots and corresponding quantification of RAGE in ventricular tissues(n = 4). **(J–K)** Representative immunoblots and corresponding quantification of RAGE in NRCMs(n = 4). Data was calculated by one-way analysis of variance (Tukey's multiple comparisons test). $^{*}P < 0.05$, $^{**}P < 0.01$.

provide a potential therapeutic strategy to improve mitochondrial energy metabolism in DCM.

DCM is a diabetes-induced pathophysiological condition characterized by early diastolic dysfunction, which gradually progresses to systolic dysfunction as diabetes advances. Recent studies have reported reduced LVEF and E/A ratio in diabetic mice, suggesting impaired cardiac systolic and diastolic function following STZ administration [18,19]. Interestingly, in db/db mice, the E/A ratio significantly increases, indicating impaired diastolic function [20]. This discrepancy likely arises from the timing of cardiac function assessment. In the early stages of diastolic dysfunction, impaired left ventricular relaxation leads to a decreased E/A ratio. However, as the disease progresses to the restrictive filling stage, increased ventricular stiffness and fibrosis result in an increased E/A ratio. In this study, we observed a decreased E/A ratio in diabetic mice, likely due to the relatively early timing of cardiac function assessment. This phenomenon was more pronounced in mice with cardiomyocyte-specific USP38 overexpression. In contrast, cardiomyocyte-specific USP38 knockout improved the E/A ratio and diastolic function in diabetic mice. Notably, no significant changes in blood glucose levels were observed, suggesting that USP38 promotes pathological cardiac remodeling in diabetic mice through directly targeting, rather than through glycemic control.

DCM is driven by diverse pathological cardiac remodeling processes. Among these, structural and electrical remodeling have received the most research attention [18,21,22]. Structural remodeling, manifested by the development of myocardial fibrosis and inflammation, leads to

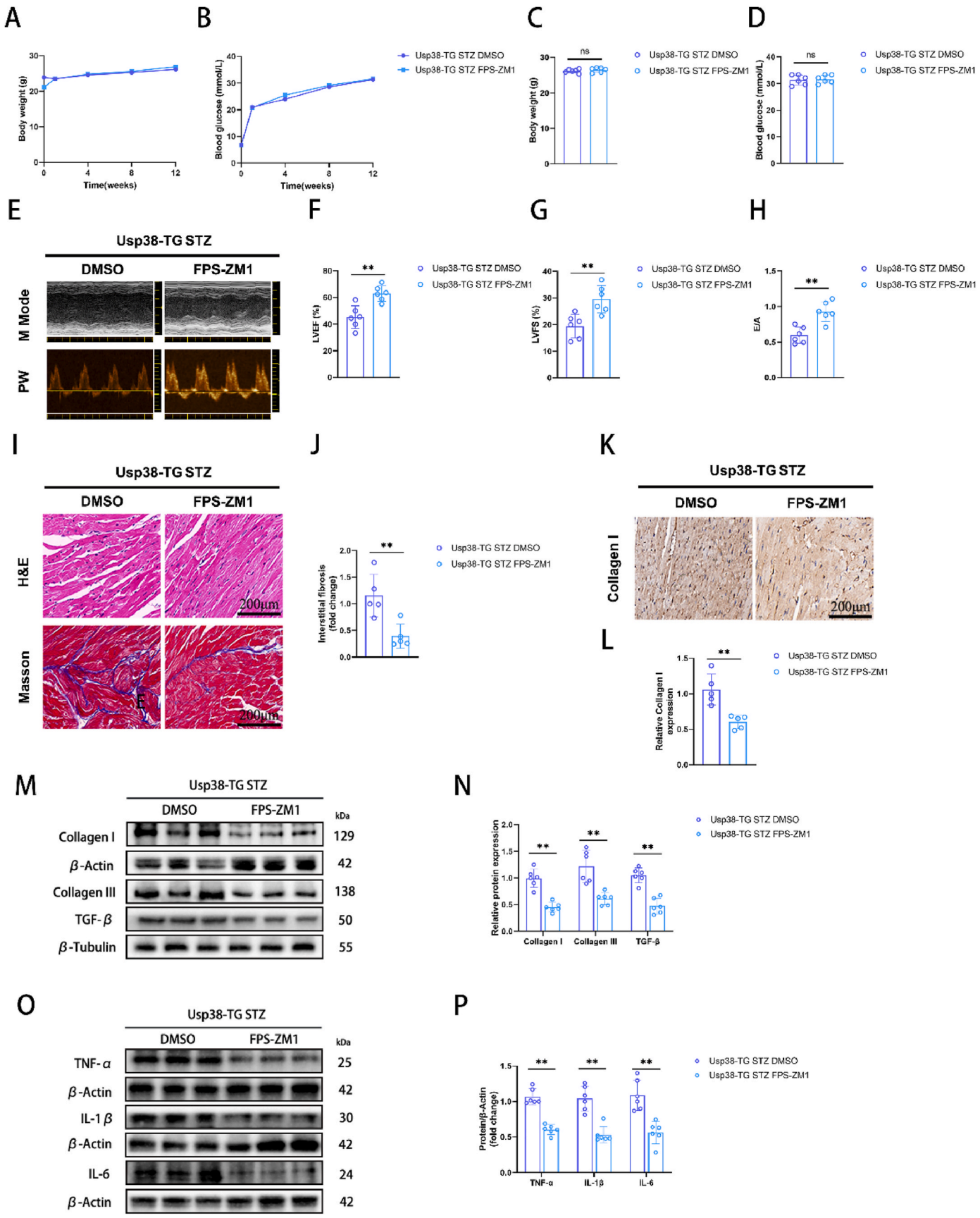


*(caption on next page)*

**Fig. 10.** FPS-ZM1 improves cardiac function and cardiac structural remodeling in Usp38-TG diabetic mice.
**(A)** Change in body weight in each group after 0w, 1w, 4w, 8w and 12w (n = 6–7). **(B)** Statistical analysis of body weight in each group after 12 w (n = 6–7). **(C)** Change in blood glucose in each group after 0w, 1w, 4w, 8w and 12w (n = 6–7). **(D)** Statistical analysis of blood glucose in each group after 12 w (n = 6–7). **(E–H)** Representative images and corresponding quantification of echocardiography (n = 6–7). **(I–J)** Representative images of H&E stained and Masson stained, and corresponding quantification based on myocardial fibrosis (magnification × 40) (n = 6). **(K–L)** Representative immunohistochemical images and corresponding quantification of Collagen I (magnification × 40) (n = 6). **(M–N)** Representative immunoblots and corresponding quantification for Collagen I, Collagen III and TGF-β(n = 4). **(O–P)** Representative immunoblots and corresponding quantification for TNF-α, IL-1-β and IL-6 (n = 4). Data was calculated by student's *t*-test (unpaired, two-tailed, two groups). $^{*}P < 0.05$, $^{**}P < 0.01$.

cardiac dysfunction [23]. Notably, STZ administration promotes collagen accumulation in the cardiac interstitial space [18,19]. Our team has previously demonstrated that USP38 overexpression increases collagen synthesis in hearts subjected to pressure overload-induced heart failure [14]. Moreover, increased expression of inflammatory cytokines in diabetic mice indicates that inflammation plays a key role in DCM progression [19]. Our recent study also confirmed that USP38 accelerates atrial remodeling and increases vulnerability to atrial fibrillation by promoting inflammation [24]. In this study, we observed significant myocardial fibrosis and inflammation in diabetic mice, with more pronounced collagen protein deposition and inflammatory cytokine expression in Usp38-TG diabetic mice. In contrast, cardiomyocyte-specific USP38 deficiency reduced collagen expression and improved cardiac inflammation. This finding suggests that USP38 promotes cardiac structural remodeling in diabetic mice.

Cardiac electrical remodeling, which is associated with abnormal ion channel function and expression, significantly contributes to increased susceptibility to VAs. Reduced transient outward potassium current ($I_{to}$) is a key factor leading to prolonged APD and QT intervals, both critical contributors to VAs. Numerous studies have demonstrated that diabetic mice exhibit prolonged APD and QT intervals, alongside increased vulnerability to VAs, primarily due to a reduction in $I_{to}$ [22,25]. Previous study has also shown that USP38 overexpression prolongs APD and QT intervals, increasing the induration rate of VAs in heart failure models [26]. Our findings are consistent with the previous study, we observed that cardiomyocyte-specific USP38 overexpression exacerbated electrical instability, manifested by prolonged QT intervals and APD90, as well as increased susceptibility to VAs. This may due to the reduced expression of Kv4.2 and Kv4.3, key ion channels involved cardiac repolarization. Thus, USP38 promotes cardiac electrical remodeling in diabetic mice by influencing the protein expression of potassium ion channels.

Recent research has increasingly highlighted the role of cardiac metabolic remodeling in DCM. Metabolic remodeling occurs early, often preceding cardiac structural and electrical changes [6]. In diabetic states, cardiomyocytes exhibit a metabolic shift, manifested by increased fatty acids and decreased glucose utilization for ATP production [7,27,28]. Thus, regulating fatty acids oxidation is particularly important in DCM. However, over time, fatty acid oxidation fails to adequately metabolize all intracellular fatty acids, leading to cardiac lipotoxicity [7,27,28]. Previous studies have demonstrated increased lipid deposition and cardiac lipotoxicity in db/db mouse models and STZ/high fat diet (HFD) mouse models [20,29,30]. Similarly, other studies have reported increased cardiac lipotoxicity in STZ-induced diabetic models [27,31]. In the present study, lipidomic analysis revealed elevated levels of toxic lipids, such as diacylglycerols and triglycerides, in Usp38-TG diabetic hearts. Notably, although Oil Red staining did not reveal significant lipid accumulation in the hearts of diabetic mice, transmission electron microscopy identified the presence of lipid droplets. As previously reported, both type 1 diabetes and type 2 diabetes develop metabolic abnormalities in the myocardium, primarily characterized by increased fatty acid uptake and oxidation [29,31]. In comparison to type 2 diabetes models, type 1 diabetes animal models, lacking the effects of high-fat feeding, exhibit a slower lipid deposition progression. Consequently, lipid droplets were only detectable at the microscopic level in our study.

Mitochondria occupy a central role in energy production. In DCM animal models, mitochondrial dysfunction is manifested by morphological alteration, decreased mitochondrial membrane potential, and ROS overproduction. In our study, we observed that cardiomyocyte-specific USP38 overexpression aggravates mitochondrial morphofunctional defects in diabetic mice. As a member of the deubiquitinating enzymes family, USP38 has been implicated in cardiovascular diseases. For example, USP38 promotes heart failure progression and increases susceptibility to VAs by deubiquitinating phospho-TANK-binding kinase 1 [14,26]. Moreover, USP38 accelerates ferroptosis by removing K48-linked polyubiquitination chain from iron regulatory protein 2 in diabetic hearts, accompanied by increased induction rate of atrial fibrillation [16]. Notably, recent studies have also reported the role of USP38 in other ubiquitin linkage types, such as K63-linked, K11-linked and K33-linked ubiquitination [15,32,33]. In our study, we demonstrated that USP38 serves as a deubiquitinating enzyme regulatingACAD11 activation. ACAD11 primarily utilizes long-chain fatty acids in mitochondrial fatty acid β-oxidation in human neuroblastoma cells. Recently, Paquay et al. found that ACAD11 is localized in peroxisomes and engaged in hydroxy fatty acids β-oxidation [12]. In our study, we found that ACAD11 is located in both mitochondria and peroxisomes, suggesting its involvement in fatty acid β-oxidation in multiple organelles. Additionally, we observed that the C domain of USP38 directly interacts with the APH domain of ACAD11. Notably, in NG-treated NRCMs, although USP38 influenced the ubiquitination level of ACAD11, it did not significantly affect ATP production. However, in HG-treated NRCMs, USP38 further reduced ATP production by decreasing the ubiquitination level of ACAD11. Therefore, we speculate that ACAD11 may act as a backup system for fatty acid oxidation in normal cardiomyocytes, compensating for other members of the ACADs family.

Previous studies have positioned RAGE at the center of DCM pathogenesis [34]. RAGE, a pattern recognition receptor expressed in cardiomyocytes, interacts with multiple ligands, initiating a series of events that lead to myocardial damage, including inflammation, extracellular matrix accumulation, oxidation stress, and apoptosis, etc [34–36]. In our study, we found that the USP38-ACAD11 axis mediated fatty acids metabolism disorder is linked to the AGE-RAGE signaling pathway through lipidomic analysis and RNA sequencing analysis. We further demonstrated that USP38 promotes RAGE activation in diabetic hearts. Inhibition of RAGE has been shown to improve diabetic cardiac remodeling by inactivating the NF-κB signaling pathway and reducing ROS production [35]. Similarly, calcitriol has been reported to relieve cardiac fibrosis by downregulating RAGE expression [36]. Consistent with these reports, we discovered that inhibition of RAGE by FPS-ZM1 improved cardiac function and alleviated inflammation, fibrosis in Usp38-TG diabetic hearts, indicating that USP38 promotes cardiac remodeling via the RAGE pathway in diabetic mice.

This study has several limitations. For animal-related aspects, as female mice are less sensitive to STZ than male mice, leading to a lower model-establishment success rate, only male mice were used in this study. Further research should include experiments on female mice. Regarding the number of animals, although conclusions were drawn from the existing sample size, ethical guidelines restricted us from increasing the number. In futhre studies, we will determine an appropriate number while following animal ethics. In terms of molecular mechanism, while the binding between USP38 domain and ACAD11 domain is confirmed, the specific deubiquitination function of USP38 on

ACAD11's lysine residues remain unclear. Also, although we have determined that USP38 removes the K63-linked polyubiquitin chain from ACAD11, but we did not investigate other polyubiquitin chain modifications. Further exploration is needed to clarify the precise mechanism of USP38 on ACAD11.

## 5. Conclusion

In conclusion, our study underscores the pivotal role of USP38 in the pathogenesis of DCM. We demonstrate that USP38 expression is upregulated in DCM, and cardiomyocyte-specific overexpression of USP38 exacerbates cardiac remodeling in diabetic mice. Mechanistically, USP38 removes the K63-linked polyubiquitin chain from ACAD11, thereby impairing lipid metabolism and inducing mitochondrial dysfunction. These alterations subsequently activate the RAGE signaling pathway. Thus, therapeutic targeting of the USP38-ACAD11-RAGE axis may represent a promising strategy for the treatment of DCM.

## CRediT authorship contribution statement

**Zheng Xiao:** Methodology, Project administration, Writing – original draft, Writing – review & editing. **Yucheng Pan:** Conceptualization, Data curation, Formal analysis, Project administration, Software. **Hong Meng:** Investigation, Methodology. **Zongze Qu:** Investigation, Methodology, Software. **Liang Guo:** Resources, Software, Validation. **Bin Kong:** Investigation, Validation, Visualization. **Wei Shuai:** Funding acquisition, Supervision, Validation. **He Huang:** Funding acquisition, Resources, Supervision, Visualization.

## Funding

This work was supported by grants from National Natural Science Foundation of China (No.82200348, 82070330).

## Declaration of competing interest

We are pleased to submit the enclosed manuscript titled "Ubiquitin - specific protease 38 exacerbates diabetic cardiomyopathy via post - translational modification of ACAD11" for potential publication in "Redox Biology". We confirm that there are no conflicts of interest associated with the submission of this manuscript. All the authors have thoroughly reviewed and approved the manuscript for publication.

On behalf of all co-authors, I hereby declare that the research presented in this manuscript is original. It has not been previously published in any form, nor is it currently under consideration for publication in any other journal, either in its entirety or in part. Each of the listed authors has given their consent for the submission of this enclosed manuscript.

## Acknowledgements

We thank Dr. Yang Hongjie and Dr. Wang Yuhui for the assistant they provided throughout the entire experimental process.

## Appendix A. Supplementary data

Supplementary data to this article can be found online at https://doi.org/10.1016/j.redox.2025.103704.

## References

[1] G.A. Gregory, T.I.G. Robinson, S.E. Linklater, F. Wang, S. Colagiuri, C. de Beaufort, K.C. Donaghue, , International Diabetes Federation Diabetes Atlas Type 1 Diabetes in Adults Special Interest G, D.J. Magliano, J. Maniam, Global incidence, prevalence, and mortality of type 1 diabetes in 2021 with projection to 2040: a modelling study, Lancet Diabetes Endocrinol. 10 (10) (2022) 741–760, https://doi.org/10.1016/S2213-8587(22)00218-2.

[2] M. Haji, S. Erqou, G.C. Fonarow, J.B. Echouffo-Tcheugui, Type 1 diabetes and risk of heart failure: a systematic review and meta-analysis, Diabetes Res. Clin. Pract. 202 (2023) 110805, https://doi.org/10.1016/j.diabres.2023.110805.

[3] T. Ohkuma, Y. Komorita, S.A.E. Peters, M. Woodward, Diabetes as a risk factor for heart failure in women and men: a systematic review and meta-analysis of 47 cohorts including 12 million individuals, Diabetologia (Berl.) 62 (9) (2019) 1550–1560, https://doi.org/10.1007/s00125-019-4926-x.

[4] J. Guo, T. Costacou, T.J. Orchard, Long term risk of heart failure in individuals with childhood-onset type 1 diabetes, J Diabetes Complications 36 (8) (2022) 108233, https://doi.org/10.1016/j.jdiacomp.2022.108233.

[5] P. Chakraborty, S. Nattel, K. Nanthakumar, K.A. Connelly, M. Husain, S.S. Po, Ha ACT: sudden cardiac death due to ventricular arrhythmia in diabetes mellitus: a bench to bedside review, Heart Rhythm 21 (10) (2024) 1827–1837, https://doi.org/10.1016/j.hrthm.2024.05.063.

[6] G. Jia, M.A. Hill, J.R. Sowers, Diabetic cardiomyopathy: an Update of mechanisms contributing to this clinical entity, Circ. Res. 122 (4) (2018) 624–638, https://doi.org/10.1161/CIRCRESAHA.117.311586.

[7] T. Yamamoto, M. Sano, Deranged myocardial fatty acid metabolism in heart failure, Int. J. Mol. Sci. 23 (2) (2022), https://doi.org/10.3390/ijms23020996.

[8] P. Herrero, L.R. Peterson, J.B. McGill, S. Matthew, D. Lesniak, C. Dence, R. J. Gropler, Increased myocardial fatty acid metabolism in patients with type 1 diabetes mellitus, J. Am. Coll. Cardiol. 47 (3) (2006) 598–604, https://doi.org/10.1016/j.jacc.2005.09.030.

[9] Z. Swigonova, A.W. Mohsen, J. Vockley, Acyl-CoA dehydrogenases: dynamic history of protein family evolution, J. Mol. Evol. 69 (2) (2009) 176–193, https://doi.org/10.1007/s00239-009-9263-0.

[10] S.M. Houten, S. Violante, F.V. Ventura, R.J. Wanders, The biochemistry and physiology of mitochondrial fatty acid beta-oxidation and its genetic disorders, Annu. Rev. Physiol. 78 (2016) 23–44, https://doi.org/10.1146/annurev-physiol-021115-105045.

[11] M. He, Z. Pei, A.W. Mohsen, P. Watkins, G. Murdoch, P.P. Van Veldhoven, R. Ensenauer, J. Vockley, Identification and characterization of new long chain acyl-CoA dehydrogenases, Mol Genet Metab 102 (4) (2011) 418–429, https://doi.org/10.1016/j.ymgme.2010.12.005.

[12] S. Paquay, J. Duraffourd, M. Bury, I.P. Heremans, F. Caligiore, I. Gerin, V. Stroobant, J. Jacobs, A. Pinon, J. Graff, et al., ACAD10 and ACAD11 allow entry of 4-hydroxy fatty acids into beta-oxidation, Cell. Mol. Life Sci. 81 (1) (2024) 367, https://doi.org/10.1007/s00018-024-05397-8.

[13] K.N. Swatek, D. Komander, Ubiquitin modifications, Cell Res. 26 (4) (2016) 399–422, https://doi.org/10.1038/cr.2016.39.

[14] Z. Xiao, C. Dai, T. Yu, J. Zhu, Y. Pan, W. Shuai, B. Kong, H. Huang, Ubiquitin specific protease 38 aggravates pathological cardiac remodeling by stabilizing phospho-TBK1, Int. J. Biol. Sci. 20 (5) (2024) 1815–1832, https://doi.org/10.7150/ijbs.85562.

[15] Y. Yang, C. Yang, T. Li, S. Yu, T. Gan, J. Hu, J. Cui, X. Zheng, The deubiquitinase USP38 promotes NHEJ repair through regulation of HDAC1 activity and regulates cancer cell response to genotoxic insults, Cancer Res. 80 (4) (2020) 719–731, https://doi.org/10.1158/0008-5472.CAN-19-2149.

[16] Z. Xiao, H. Yang, Y. Pan, H. Meng, Z. Qu, B. Kong, W. Shuai, H. Huang, Ubiquitin-specific protease 38 promotes atrial fibrillation in diabetic mice by stabilizing iron regulatory protein 2, Free Radic. Biol. Med. (2024), https://doi.org/10.1016/j.freeradbiomed.2024.08.021.

[17] M.T. Julian, A. Perez-Montes de Oca, J. Julve, N. Alonso, The double burden: type 1 diabetes and heart failure-a comprehensive review, Cardiovasc. Diabetol. 23 (1) (2024) 65, https://doi.org/10.1186/s12933-024-02136-y.

[18] L. Meng, Y. Lu, X. Wang, C. Cheng, F. Xue, L. Xie, Y. Zhang, W. Sui, M. Zhang, Y. Zhang, et al., NPRC deletion attenuates cardiac fibrosis in diabetic mice by activating PKA/PKG and inhibiting TGF-beta1/Smad pathways, Sci. Adv. 9 (31) (2023) eadd4222, https://doi.org/10.1126/sciadv.add4222.

[19] Z. Guo, H. Tuo, N. Tang, F.Y. Liu, S.Q. Ma, P. An, D. Yang, M.Y. Wang, D. Fan, Z. Yang, et al., Neuraminidase 1 deficiency attenuates cardiac dysfunction, oxidative stress, fibrosis, inflammatory via AMPK-SIRT3 pathway in diabetic cardiomyopathy mice, Int. J. Biol. Sci. 18 (2) (2022) 826–840, https://doi.org/10.7150/ijbs.65938.

[20] S.Y. Xie, S.Q. Liu, T. Zhang, W.K. Shi, Y. Xing, W.X. Fang, M. Zhang, M.Y. Chen, S. C. Xu, M.Q. Fan, et al., USP28 serves as a key suppressor of mitochondrial morphofunctional defects and cardiac dysfunction in the diabetic heart, Circulation (New York, N. Y.) 149 (9) (2024) 684–706, https://doi.org/10.1161/CIRCULATIONAHA.123.065603.

[21] F. Xue, J. Cheng, Y. Liu, C. Cheng, M. Zhang, W. Sui, W. Chen, P. Hao, Y. Zhang, C. Zhang, Cardiomyocyte-specific knockout of ADAM17 ameliorates left ventricular remodeling and function in diabetic cardiomyopathy of mice, Signal Transduct Target Ther 7 (1) (2022) 259, https://doi.org/10.1038/s41392-022-01054-3.

[22] D.S. Li, G.L. Xue, J.M. Yang, C.Z. Li, R.X. Zhang, T. Tian, Z. Li, K.W. Shen, Y. Guo, X.N. Liu, et al., Knockout of interleukin-17A diminishes ventricular arrhythmia susceptibility in diabetic mice via inhibiting NF-kappaB-mediated electrical remodeling, Acta Pharmacol. Sin. 43 (2) (2022) 307–315, https://doi.org/10.1038/s41401-021-00659-8.

[23] Y. Tan, Z. Zhang, C. Zheng, K.A. Wintergerst, B.B. Keller, L. Cai, Mechanisms of diabetic cardiomyopathy and potential therapeutic strategies: preclinical and clinical evidence, Nat. Rev. Cardiol. 17 (9) (2020) 585–607, https://doi.org/10.1038/s41569-020-0339-2.

[24] Z. Xiao, Y. Pan, B. Kong, H. Meng, W. Shuai, H. Huang, Ubiquitin-specific protease 38 promotes inflammatory atrial fibrillation induced by pressure overload,

Europace (Lond., Engl.) 26 (1) (2023), https://doi.org/10.1093/europace/euad366.
[25] M. Meo, O. Meste, S. Signore, A. Sorrentino, A. Cannata, Y. Zhou, A. Matsuda, M. Luciani, R. Kannappan, P. Goichberg, et al., Reduction in Kv current enhances the temporal dispersion of the action potential in diabetic myocytes: insights from a novel repolarization algorithm, J. Am. Heart Assoc. 5 (2) (2016), https://doi.org/10.1161/JAHA.115.003078.
[26] Y. Pan, Z. Xiao, H. Yang, B. Kong, H. Meng, W. Shuai, H. Huang, USP38 exacerbates pressure overload-induced left ventricular electrical remodeling, Mol Med 30 (1) (2024) 97, https://doi.org/10.1186/s10020-024-00846-3.
[27] R.H. Ritchie, E.J. Zerenturk, D. Prakoso, A.C. Calkin, Lipid metabolism and its implications for type 1 diabetes-associated cardiomyopathy, J. Mol. Endocrinol. 58 (4) (2017) R225–R240, https://doi.org/10.1530/JME-16-0249.
[28] Q.G. Karwi, Q. Sun, G.D. Lopaschuk, The contribution of cardiac fatty acid oxidation to diabetic cardiomyopathy severity, Cells-Basel 10 (11) (2021), https://doi.org/10.3390/cells10113259.
[29] H. Wang, J. Wang, H. Cui, C. Fan, Y. Xue, H. Liu, H. Li, J. Li, H. Li, Y. Sun, et al., Inhibition of fatty acid uptake by TGR5 prevents diabetic cardiomyopathy, Nat. Metab. 6 (6) (2024) 1161–1177, https://doi.org/10.1038/s42255-024-01036-5.
[30] M. Wu, J. Tan, Z. Cao, Y. Cai, Z. Huang, Z. Chen, W. He, X. Liu, Y. Jiang, Q. Gao, et al., Sirt5 improves cardiomyocytes fatty acid metabolism and ameliorates cardiac lipotoxicity in diabetic cardiomyopathy via CPT2 de-succinylation, Redox Biol. 73 (2024) 103184, https://doi.org/10.1016/j.redox.2024.103184.
[31] I.D. Kyriazis, M. Hoffman, L. Gaignebet, A.M. Lucchese, E. Markopoulou, D. Palioura, C. Wang, T.D. Bannister, M. Christofidou-Solomidou, S.I. Oka, et al., KLF5 is induced by FOXO1 and causes oxidative stress and diabetic cardiomyopathy, Circ. Res. 128 (3) (2021) 335–357, https://doi.org/10.1161/CIRCRESAHA.120.316738.
[32] R. Wang, X. Cai, X. Li, J. Li, X. Liu, J. Wang, W. Xiao, USP38 promotes deubiquitination of K11-linked polyubiquitination of HIF1alpha at Lys769 to enhance hypoxia signaling, J. Biol. Chem. 300 (1) (2024) 105532, https://doi.org/10.1016/j.jbc.2023.105532.
[33] M. Lin, Z. Zhao, Z. Yang, Q. Meng, P. Tan, W. Xie, Y. Qin, R.F. Wang, J. Cui, USP38 inhibits type I interferon signaling by editing TBK1 ubiquitination through NLRP4 signalosome, Mol Cell 64 (2) (2016) 267–281, https://doi.org/10.1016/j.molcel.2016.08.029.
[34] V.L. Bodiga, S.R. Eda, S. Bodiga, Advanced glycation end products: role in pathology of diabetic cardiomyopathy, Heart Fail. Rev. 19 (1) (2014) 49–63, https://doi.org/10.1007/s10741-013-9374-y.
[35] H.H. Xu, S.X. Hao, H.Y. Sun, X.X. Dong, Y. Lin, H. Lou, L.M. Zhao, P.P. Tang, Z. J. Dou, J.J. Han, et al., THBru attenuates diabetic cardiomyopathy by inhibiting RAGE-dependent inflammation, Acta Pharmacol. Sin. 45 (10) (2024) 2107–2118, https://doi.org/10.1038/s41401-024-01307-7.
[36] T.W. Lee, Y.H. Kao, T.I. Lee, C.J. Chang, G.S. Lien, Y.J. Chen, Calcitriol modulates receptor for advanced glycation end products (RAGE) in diabetic hearts, Int. J. Cardiol. 173 (2) (2014) 236–241, https://doi.org/10.1016/j.ijcard.2014.02.041.